Myoplasmic Calcium Transients Monitored with Purpurate Indicator Dyes Injected into Intact Frog Skeletal Muscle Fibers

M. KONISHI and S. M. BAYLOR

From the Department of Physiology, University of Pennsylvania Medical Center, Philadelphia, Pennsylvania 19104-6085

ABSTRACT Intact single twitch fibers from frog muscle were studied on an optical bench apparatus after microinjection with tetramethylmurexide (TMX) or purpurate-3,3′diacetic acid (PDAA), two compounds from the purpurate family of absorbance Ca^{2+} indicators previously used in cut muscle fibers (Maylie, J., M. Irving, N. L. Sizto, G. Boyarsky, and W. K. Chandler. 1987. *J. Gen. Physiol.* 89:145–176; Hirota, A., W. K. Chandler, P. L. Southwick, and A. S. Waggoner. 1989. *J. Gen. Physiol.* 94:597–631.) The apparent longitudinal diffusion constant of PDAA (mol wt 380) in myoplasm was 0.99 (±0.04, SEM) × 10^{-6} cm^2 s^{-1} (16–17°C), a value which suggests that 24–43% of the PDAA molecules were bound to myoplasmic constituents of large molecular weight. The corresponding values for TMX (mol wt 322) were 0.98 (±0.05) × 10^{-6} cm^2 s^{-1} and 44–50%, respectively. Muscle membranes (surface and/or transverse-tubular) appear to be permeable to TMX and, to a lesser extent, to PDAA, since the total amount of indicator contained within a fiber decreased with time after injection. The average time constants for disappearance of indicator were 46 (±7, SEM) min for TMX and 338 (±82) min for PDAA. The fraction of indicator in the Ca^{2+}-bound state in resting fibers was significantly different from zero for TMX (0.070 ± 0.008) but not for PDAA (0.026 ± 0.009). In in vitro calibrations PDAA but not TMX appeared to react with Ca^{2+} with 1:1 stoichiometry. In agreement with Hirota et al. (Hirota, A., W. K. Chandler, P. L. Southwick, and A. S. Waggoner. 1989. *J. Gen. Physiol.* 94:597–631), we conclude that PDAA is probably a more reliable myoplasmic Ca^{2+} indicator than TMX. In fibers that contained PDAA and were stimulated by a single action potential, the calibrated peak value of the myoplasmic free $[Ca^{2+}]$ transient ($\Delta[Ca^{2+}]$) averaged 9.4 (±0.6) μM, a value about fivefold larger than that calibrated with antipyrylazo III under otherwise identical conditions (Baylor, S. M., and S. Hollingworth. 1988. *J. Physiol.* 403:151–192). The fivefold difference is similar to that previously reported in cut

Address reprint requests to Dr. S. M. Baylor, Department of Physiology, University of Pennsylvania Medical Center, Philadelphia, PA 19104-6085.

Dr. Konishi's current address is Department of Physiology, The Jikei University School of Medicine, 3-25-8 Nishishinbashi, Minato-Ku, Tokyo 105, Japan.

J. GEN. PHYSIOL. © The Rockefeller University Press · 0022-1295/91/02/0245/26 $2.00
Volume 97 February 1991 245–270

fibers with antipyrylazo III and PDAA. Since in both intact and cut fibers the percentage of PDAA bound to myoplasmic constituents is considerably smaller than that found for antipyrylazo III, the PDAA calibration of $\Delta[Ca^{2+}]$ is likely to be more accurate. Interestingly, in intact fibers the peak value of $\Delta[Ca^{2+}]$ calibrated with either PDAA or antipyrylazo III is about half that calibrated in cut fibers. The source of this latter difference is unclear, but one possibility is that $\Delta[Ca^{2+}]$ in cut fibers may be abnormally large because of some alteration in the internal state of these fibers.

INTRODUCTION

Purpurate Ca^{2+} indicator dyes such as tetramethylmurexide (TMX), purpurate-3,3′diacetic acid (PDAA), and 1,1′-dimethylpurpurate-3,3′diacetic acid (DMPDAA) have been successfully used in cut twitch fibers from frog muscle to monitor the myoplasmic free $[Ca^{2+}]$ transient ($\Delta[Ca^{2+}]$) in response to electrically stimulated activity (Maylie et al., 1987*c*; Hirota et al., 1989). These low affinity absorbance indicators (dissociation constants for Ca^{2+} near or exceeding 1 mM) have some significant advantages compared with higher affinity indicators previously used to monitor $\Delta[Ca^{2+}]$ in skeletal muscle. First, the optical changes from PDAA and DMPDAA, and a component of the change from TMX, appear to track $\Delta[Ca^{2+}]$ in a linear fashion and without kinetic delay. This is an important finding since the signals from the higher affinity indicators, such as arsenazo III, antipyrylazo III, azo-1, and fura-2, required kinetic corrections to accurately estimate the time course of $\Delta[Ca^{2+}]$ (Baylor et al., 1983, 1985; Hollingworth and Baylor, 1986; Baylor and Hollingworth, 1988; Klein et al., 1988). Second, with the purpurate dyes the percentage of indicator that appeared to be bound to myoplasmic constituents was relatively small (19–33%) in comparison with the major bound fraction (~60–90%) detected with the other indicators (Baylor et al., 1986; Maylie et al., 1987*a*, *b*; Baylor and Hollingworth, 1988; Konishi et al., 1988). This finding is important since an indicator with a smaller bound fraction is likely to yield a more reliable estimate of the amplitude of $\Delta[Ca^{2+}]$.

Interestingly, in cut fibers stimulated by a single action potential, the calibrated peak amplitude of $\Delta[Ca^{2+}]$ as recorded with each of the three purpurate indicators was ~20 μM (16–18°C; sarcomere length, 3.6–4.0 μm; Maylie et al., 1987*c*; Hirota et al., 1989), a value almost an order of magnitude larger than that calibrated with antipyrylazo III under otherwise indentical conditions (3.1 μM; Maylie et al., 1987*b*). A 20-μM Ca^{2+} transient is also about an order of magnitude larger than the 1–2-μM range previously calibrated from intact frog fibers with azo-1, antipyrylazo III, and fura-2 (Hollingworth and Baylor, 1986; Baylor and Hollingworth, 1988). Because of the advantages reported in cut fibers for measuring $\Delta[Ca^{2+}]$ with purpurate indicators, we wished to study the signals from these indicators in intact fibers, with a particular interest in the calibrated amplitude of $\Delta[Ca^{2+}]$.

We have found that in intact fibers injected with PDAA and stimulated by a single action potential, the calibrated peak value of $\Delta[Ca^{2+}]$ is 9.4 (±0.6, SEM) μM (16–16.5°C; sarcomere length, 3.8–4.1 μm), a value about half that reported in cut fibers. This twofold difference is due primarily to the fact that the recorded absorbance change (ΔA) per unit dye concentration is smaller in intact fibers than in cut fibers; a minor (~10%) portion of the difference is related to the value of the Ca^{2+}-PDAA dissociation constant measured under in vitro conditions (0.87 mM in

this article, 0.95 mM in Hirota et al., 1989). With TMX, our estimated value for the peak amplitude of $\Delta[Ca^{2+}]$, 13–18 μM, is also smaller than that reported in cut fibers, 17–26 μM (Maylie et al., 1987*c*). However, in the case of TMX, all of the difference in peak $\Delta[Ca^{2+}]$ can be attributed to differences in the calibration procedure itself rather than differences in the raw ΔA measurement.

In agreement with Maylie et al. (1987*c*) and Hirota et al. (1989) we conclude that: (*a*) for a variety of reasons, PDAA is a simpler and more reliable Ca^{2+} indicator than is TMX; and (*b*) the peak of $\Delta[Ca^{2+}]$ in frog twitch fibers is probably considerably larger than that calibrated previously from the higher affinity (and more highly bound) indicators. A new conclusion suggested by our results (and also supported by a comparison of earlier results obtained with antipyrylazo III; cf. Discussion) is that the peak of $\Delta[Ca^{2+}]$ in cut fibers is about twice that in intact fibers.

Additional information concerning the time course and peak value of $\Delta[Ca^{2+}]$ in intact fibers is presented in the following paper (Konishi et al., 1991), which describes the use of the fluorescent indicator furaptra (Raju et al., 1989) to monitor $\Delta[Ca^{2+}]$ in response to action potential stimulation.

METHODS

This article describes in vitro and in vivo measurements carried out with PDAA (Southwick and Waggoner, 1989) and TMX. DMPDAA was not used as the results obtained in cut fibers with DMPDAA (Hirota et al., 1989) were quite similar to those obtained with PDAA.

In Vitro Calibrations with PDAA and TMX

In general, calibration of an indicator-related ΔA in terms of $\Delta[Ca^{2+}]$ depends on assumptions made about the stoichiometry of the Ca^{2+}-indicator reaction, the dissociation constant(s) of the relevant reaction(s), and the values of extinction coefficient that apply to the Ca^{2+}-free and Ca^{2+}-bound forms of the indicator. In the case of purpurate indicators, previous reports have assumed a 1:1 Ca^{2+}-indicator stoichiometry for both TMX (Ohnishi, 1978; Ogawa et al., 1980; Maylie et al., 1987*c*) and PDAA (Hirota et al., 1989). However, Maylie et al. (1987*c*), in their in vitro calibrations, noted that the apparent dissociation constant (K_d) of TMX for Ca^{2+} decreased by 10–12% as indicator concentration increased from 0.025 to 0.5 mM, an effect not expected for 1:1 stoichiometry. The possibility of an analogous effect in the case of PDAA was not tested by Hirota et al. (1989), who used only a low indicator concentration (0.03 mM) in their in vitro measurements.

Since millimolar concentrations of both indicators were used in our intact muscle fiber experiments, it was important to obtain additional information about the in vitro properties of the Ca^{2+}-indicator reaction(s) at millimolar concentrations of the indicators. For our in vitro calibrations a standard salt solution was used, containing (in mM): 120 KCl, 10 NaCl, and 10 PIPES (piperazine-*N*,*N*′-bis[2-ethane sulphonic acid]), titrated with KOH at room temperature (21–24°C) to pH 6.90. PDAA and TMX were added to final concentrations of 0.04–2 mM. PDAA (tripotassium salt) from a batch different from that used by Hirota et al. (1989) was a generous gift of Dr. W. K. Chandler. TMX (ammonium salt; lot Nos. 584401 and 607702) was obtained from Calbiochem Corp. (La Jolla, CA). Contamination of Ca^{2+} in the TMX sample was checked in one sample (lot 607702) by means of a Ca^{2+}-selective electrode and found to be very small: no more than 0.0002 mol/mol.

The in vitro absorbance measurements were carried out at 17°C in a UV-visible spectrophotometer (model 4050; LKB Instruments, Inc., Gaithersburg, MD). The digitized absorbance

data, collected in 2–4-nm steps at wavelengths λ between 450 and 700 nm, were analyzed on a computer by means of previously described procedures (Hollingworth et al., 1987). The spectral shapes obtained (cf. curves in Figs. 4 and 6) were closely similar to those given in Maylie et al. (1987*c*) and Hirota et al. (1989). For PDAA, $\epsilon_D(520)$, the extinction coefficient at 520 nm for the metal-free form of the dye, was not measured and was assumed to be the same as given in Hirota et al. (1989), 1.50×10^4 M^{-1} cm^{-1}. For TMX, $\epsilon_D(520)$ was estimated to be 1.60 (±0.01, SEM) $\times$ 10^4 M^{-1} cm^{-1}, a value closely similar to that reported by Maylie et al. (1987*c*), 1.58×10^4 M^{-1} cm^{-1}.

Titrations of PDAA and TMX with calcium. Indicator absorbance spectra $A(\lambda)$ were measured in a 0 Ca^{2+} solution (standard buffer solution with 0.1–0.4 mM added EDTA) and in the standard buffer solution plus various concentrations of added Ca^{2+}, 0.1–10 mM, obtained from a certified 1 M stock of $CaCl_2$ (BDH Chemicals Ltd., Poole, UK). Ca^{2+} difference spectra $\Delta A(\lambda)$ were generated by subtraction of the 0 Ca^{2+} spectra from the spectra obtained with added Ca^{2+}. With either dye (PDAA or TMX) the 0 Ca^{2+} spectra measured at different dye concentrations (0.04–0.92 mM PDAA, 0.10–1.96 mM TMX), if normalized by the product of indicator concentration and cuvette path length, were identical. Moreover, with either indicator all difference spectra had identical shapes, the amplitude of which increased with increasing amounts of added Ca^{2+}. These features are expected if each indicator forms a single stoichiometric complex with Ca^{2+} and does not dimerize in a 0 Ca^{2+} solution.

For quantitative analysis, the amplitudes of the Ca^{2+} difference spectra were compared with the predictions of 1:1 stoichiometry to estimate: (*a*) K_d, the apparent dissociation constant of the Ca^{2+}-dye reaction, and (*b*) $\Delta\epsilon(\lambda)$, the change in extinction coefficient of the indicator between its Ca^{2+}-free and Ca^{2+}-bound forms. For this analysis, least-squares–fitted scaling factors were determined that related the amplitude of $\Delta A(\lambda)$ measured with the largest concentration of added Ca^{2+} to that measured with the smaller concentrations of added Ca^{2+}. An iterative least-squares computer program then adjusted the values of K_d and the amplitude of $\Delta A(\lambda)$ at saturating $[Ca^{2+}]$ to best satisfy the predictions of 1:1 stoichiometry. The results of the latter fitting were expressed (cf. Fig. 1 *A*) in terms of binding curves of the form

$$f = \frac{[Ca^{2+}]}{[Ca^{2+}] + K_d}. \quad (1)$$

In Eq. 1 $[Ca^{2+}]$ denotes the free concentration of Ca^{2+} (total concentration of added Ca^{2+} minus the estimated concentration of Ca^{2+}-dye complex) and f denotes the fraction of the dye complexed with Ca^{2+} (assumed to be equal to the amplitude of any given Ca^{2+} difference spectrum divided by the estimated amplitude at saturating $[Ca^{2+}]$). According to Beer's law, the amplitude at saturation, after division by the product of path length and indicator concentration, gives $\Delta\epsilon(\lambda)$.

Ca^{2+}-PDAA. Two Ca^{2+}-PDAA titrations, at low (0.04 mM) and high (0.92 mM) indicator concentration, were carried out. In both titrations the relative amplitudes of the difference spectra (not shown) were well fitted by Eq. 1. The best-fit values of K_d were essentially identical for the two titrations, 0.87 and 0.86 mM (low and high indicator concentrations, respectively), as were the normalized amplitude changes extrapolated to saturating Ca^{2+}, which differed by $< 1\%$. From the change with saturating Ca^{2+} and the underlying shape of the Ca^{2+} difference spectrum, the change in extinction coefficient at any particular wavelength could be calculated. For example, $\Delta\epsilon(570)$, the extinction change at 570 nm, was estimated to be -0.71×10^4 M^{-1} cm^{-1}. This value is essentially the same as that reported by Hirota et al. (1989), -0.70×10^4 M^{-1} cm^{-1}. Our K_d values are also close to that given by Hirota et al. (1989), 0.95 mM, which was estimated at 0.026 mM indicator in 150 mM KCl and 10 mM PIPES (pH 7.0, 16°C). Thus, the

main new information obtained in our titrations is that, even at near millimolar concentrations of indicator, the absorbance spectra of PDAA are consistent with a 1:1 Ca^{2+}-dye stoichiometry.

Ca^{2+}-TMX. Similar titrations and fits were carried out with TMX (cf. Fig. 1 *A*). The results revealed a clear dependence of the fitted values of both K_d and $\Delta\epsilon$ on indicator concentration (cf. Fig. 1 *B*). The effect of indicator concentration on K_d was particularly noticeable. For example, an increase in the concentration of TMX from 0.10 to 1.96 mM produced a 35% decrease in the fitted value of K_d, from 2.99 to 1.94 mM; the corresponding change in $\Delta\epsilon$(570)

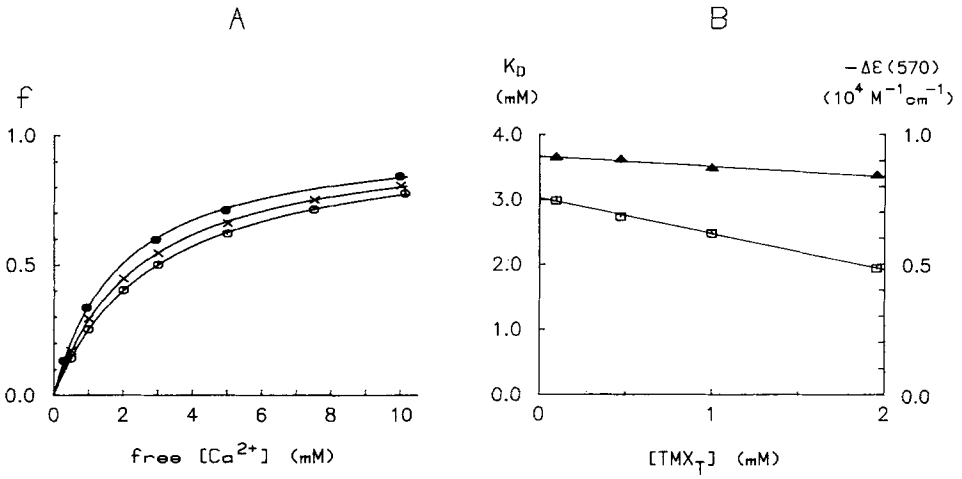

FIGURE 1. Analysis of in vitro titrations carried out with TMX. (*A*) The ordinate estimates the fraction, *f*, of the indicator in the Ca^{2+}-bound form as a function of the free Ca^{2+} concentration shown on the abscissa. To estimate *f*, the relative amplitudes of the Ca^{2+} indicator difference spectra, measured for λ between 450 and 700 nm, were fitted under the assumption of 1:1 stochiometry (cf. Eq. 1). For the fitting, the spectral amplitude at saturating [Ca^{2+}], with the latter corresponding to relative amplitude 1.0, was taken as an adjustable parameter, as was the value of K_d. The values of K_d obtained in the fits (cf. curves) were 2.99 mM (*open circles*, at 0.1 mM [TMX_T]), 2.48 mM (*crosses*, at 1.00 mM [TMX_T]), and 1.96 mM (*filled circles*, at 1.96 mM [TMX_T]). (*B*) Summary of parameter fits for the in vitro Ca^{2+}-TMX titrations of the type illustrated in *A*; data analysis was carried out as described in Methods. *Open squares*, values of K_d (left-hand ordinate) at different values of [TMX_T] (abscissa). *Filled triangles*, $-\Delta\epsilon$(570), i.e., minus the change in molar extinction coefficient of TMX at 570 nm due to Ca^{2+} binding (right hand ordinate) at different values of [TMX_T] (abscissa). The curves represent least-squares regression lines fitted to the data. The slope and *y* intercept values are, respectively, −0.553 and 3.02 mM (*open squares*) and 0.0386×10^7 M^{-2} cm^{-1} and -0.916×10^4 M^{-1} cm^{-1} (*filled triangles*).

was 8%, from −0.91 to -0.84×10^4 M^{-1} cm^{-1}. These results confirm and extend the measurements of Maylie et al. (1987*c*), who noted a 10–12% decrease in K_d, from 2.9 to 2.6 mM, for an increase in indicator concentration from 0.025 to 0.5 mM. Taken at face value, the results in Fig. 1 suggest that the Ca^{2+}-TMX reaction, in contrast to the Ca^{2+}-PDAA reaction, is not 1:1, since both the values of K_d and $\Delta\epsilon$ appear to vary with indicator concentration.

Another possible explanation for the dependencies on TMX concentration observed in Fig. 1 is that the sample of TMX was not pure. Data of the type in Fig. 1 *A* were therefore reanalyzed

to see what sample purity would be required in order for the fitted values of K_d and $\Delta\epsilon$ to be independent of TMX concentration. The analysis indicated that if the sample were only 35% TMX by weight, the fitted parameters were essentially independent of indicator concentration. However, the conclusion that 65% of the sample was made up of compounds other than TMX seems unlikely, since (*a*) the elemental analysis supplied by the distributor (Calbiochem Corp.) is consistent with an essentially pure sample, and (*b*) the chromatographic analysis of Ogawa et al. (1980), applied to a sample of TMX obtained from the same distributor, indicated a single colored substance. Thus, a more likely explanation for the concentration dependence in Fig. 1 is the existence of a higher-order stoichiometric complex, such as 1:2 (1 Ca^{2+}:2 dyes) or 2:2 (2 Ca^{2+}'s:2 dyes), or metal-free dimers. Although our absorbance data revealed no spectral evidence for another TMX complex, such complexes have been shown to exist for other Ca^{2+} indicator dyes, including arsenazo III and antipyrylazo III (Thomas, 1979; Rios and Schneider, 1981; Baylor et al., 1982*b*; Palade and Vergara, 1982; Hollingworth et al., 1987).

Because at any single value of indicator concentration the TMX ΔA data were in fact very well described by a 1:1 binding curve (although with different values of the parameters K_d and $\Delta\epsilon$ at different indicator concentrations), we have calibrated the in vivo signals (cf. last section of Methods) from the excellent empirical descriptions provided by the 1:1 binding curves and the parameter fits shown in Fig. 1.

In Vivo Measurements

The general procedure for measurement of signals from frog muscle fibers injected with indicator dyes has been described (e.g., Baylor and Hollingworth, 1988, 1990). Briefly, a single twitch fiber, dissected from a semitendinosus or ilio-fibularis muscle of a cold-adapted *Rana temporaria*, was mounted on an optical bench apparatus and stretched to long sarcomere length (3.7–4.1 μm). The Ringer's solution bathing the fiber was maintained at 16–16.5°C and contained (in mM): 120 NaCl, 2.5 KCl, 11.8 $CaCl_2$, and 5 PIPES, with pH adjusted to 7.1 by NaOH. The use of an elevated Ca^{2+} concentrated (11.8 mM, compared with the usual 1.8 mM) in the Ringer's is thought to aid fiber recovery following micro-electrode impalements (cf. De Mello, 1973), while not significantly altering the amplitude of the myoplasmic Ca^{2+} transients (Baylor and Hollingworth, 1988). Further experiments examining possible effects of the Ringer Ca^{2+} concentration on $\Delta[Ca^{2+}]$ are described in the following paper (Konishi et al., 1991).

An indicator dye, dissolved at 10–40 mM in distilled water, was pressure-injected into the myoplasm after impalement of the fiber with a dye-filled micropipette. After withdrawal of the electrode the fiber was illuminated with a small spot of quasi-monochromatic light, selected by interference filter, for the measurement of transmitted intensities (denoted by I) in the resting state and changes in transmitted intensities (denoted by ΔI) after point stimulation by brief, supra-threshold shocks from a pair of extracellular electrodes. Only fibers that responded in an all-or-none fashion for periods of many tens of minutes to several hours after injection were used in the experiments. Additionally, checks were made to verify that the injection itself did not significantly alter the fiber's responses. For this purpose, the intrinsic birefringence signal (denoted by ΔB; Baylor and Oetliker, 1977) was measured both immediately before and immediately after dye injection, as well as periodically during each experiment. Results are reported only from fibers that showed little or no change in the amplitude of the birefringence signal throughout the experiment. For example, the change in peak value of ΔB measured just after injection compared with that measured just before injection averaged −1.5% (±1.1%, SEM) for the 10 fibers injected with PDAA and −5.2% (±3.1%, SEM) for the 6 fibers injected with TMX. Since the early ΔB signal is closely related to $\Delta[Ca^{2+}]$ (Suarez-Kurtz and Parker, 1977; Baylor et al., 1982*b*; Kovacs et al., 1983; Baylor and Hollingworth, 1987; Maylie et al.,

1987*a*), the dye injection procedure probably did not significantly alter $\Delta[Ca^{2+}]$ in these experiments.

In the Results, fiber absorbance measurements obtained at different wavelengths were corrected for fiber intrinsic signals by the method previously described (e.g., Baylor et al., 1986). The analysis was based on identification of a "central" wavelength determined for each interference filter (Omega Optical Co., Brattleborough, VT), defined as the average of the two wavelengths that gave 50% of the filter's peak transmittance when measured in a spectrophotometer. For the narrow-band filters (±5-nm bandpass), central wavelengths differed from nominal wavelengths by up to 2 nm (e.g., 508 nm for the nominal 510-nm filter); for the wide-band filters (±15-nm bandpass), central wavelengths differed from nominal by up to 6 nm (e.g., 486 nm for the nominal 480-nm filter).

Constants Assumed for Calibration of the In Vivo Signals

Calibration of resting absorbance measurements in terms of total dye concentration, $[D_T]$. In dye-injected muscle fibers, $[D_T]$ was estimated from an absorbance measurement obtained with a narrow-band interference filter that had its central wavelength close to an isosbestic wavelength of the indicator. As determined in the in vitro spectrophotometer measurements (cf. curves in Fig. 6), 511 nm is an isosbestic wavelength for PDAA, and 518 nm for TMX. Thus, estimates of $[PDAA_T]$ were obtained with the narrow-band 508-nm filter, whereas those of $[TMX_T]$ were obtained with the narrow-band 521-nm filter. Beer's law was then applied, with the estimate of the optical path length in the myoplasm obtained, as previously described (Baylor et al., 1986), from the measured fiber diameter. For PDAA, $\epsilon(508)$, the extinction coefficient of the dye at 508 nm, was taken to be 1.40×10^4 M^{-1} cm^{-1}, a value appropriate for the indicator in its Ca^{2+}-free form. For TMX, selection of the appropriate value of $\epsilon(521)$ was complicated by the finding that a small fraction (average value 0.07; see Results) of TMX within the fiber appeared to be in the Ca^{2+}-bound form. Thus $\epsilon(521)$ was taken as $0.93\epsilon_D(521) + 0.07\epsilon_{CaD}(521)$ (where ϵ_D and ϵ_{CaD} refer, respectively, to the Ca^{2+}-free and Ca^{2+}-bound forms of the indicator). Although, as determined from the in vitro calibrations, values of ϵ_D were found to be essentially independent of $[TMX_T]$, values of ϵ_{CaD} did vary slightly with $[TMX_T]$ at wavelengths different from the isosbestic wavelength (cf. Fig. 1 *B*, *triangles*). However, 521 nm proved to be sufficiently close to the isosbestic wavelength (518 nm) that the values of $0.93\epsilon_D(521) + 0.07\epsilon_{CaD}(521)$ differed by $<0.5\%$ for the range of $[TMX_T]$'s encountered in the fibers, 0.4–2.0 mM. The value of $0.93\epsilon_D(521) + 0.07\epsilon_{CaD}(521)$ determined in vitro at $[TMX_T] = 1.0$ mM (namely, 1.59×10^4 M^{-1} cm^{-1}) has been used throughout the Results to estimate the in vivo values of $[TMX_T]$.

Calibration of active ΔA *signals in terms of* $\Delta[CaD]$. ΔA signals measured in response to electrical stimulation were converted to the change in concentration of Ca^{2+}-indicator complex, $\Delta[CaD]$, by means of Beer's law and an appropriately chosen extinction change, $\Delta\epsilon$. Because muscle ΔA measurements were always made with at least two dye-related wavelengths (denoted by λ_1 and λ_2), one on either side of the isosbestic wavelength, in practice "difference" ΔA's (i.e., $\Delta A(\lambda_1) - \Delta A(\lambda_2)$) were converted to $\Delta[CaD]$ by means of "difference" extinction changes (i.e., $\Delta\epsilon(\lambda_1) - \Delta\epsilon(\lambda_2)$). This procedure was chosen to minimize any errors due to improper correction of the intrinsic components in the optical records, such as might have arisen because of movement artifacts (cf. Results).

For calibration of the PDAA signals, two possible pairs of interference filters were used to calibrate $\Delta A = \Delta A(\lambda_1) - \Delta A(\lambda_2)$ by means of appropriately chosen values of $\Delta\epsilon = \Delta\epsilon(\lambda_1) -$

$\Delta\epsilon(\lambda_2)$:

wide-band 486 minus wide-band 542; $\Delta\epsilon = 2.036 \times 10^4\ M^{-1}\ cm^{-1}$

narrow-band 480 minus narrow-band 538; $\Delta\epsilon = 2.260 \times 10^4\ M^{-1}\ cm^{-1}$.

These $\Delta\epsilon$ values were taken from the in vitro spectrophotometer curves after the latter were averaged over the band-width of the particular interference filters.

With TMX, the 1:1 binding curves (cf. Fig. 1) yielded parameters that varied with indicator concentration, so that the relevant $\Delta\epsilon$'s varied slightly with $[TMX_T]$. The filter pairs and the corresponding values of $\Delta\epsilon$ appropriate to $[TMX_T] = 1.0$ mM were as follows:

wide-band 486 minus wide-band 572; $\Delta\epsilon = 2.115 \times 10^4\ M^{-1}\ cm^{-1}$

wide-band 486 minus wide-band 542; $\Delta\epsilon = 2.164 \times 10^4\ M^{-1}\ cm^{-1}$

narrow-band 480 minus narrow-band 559; $\Delta\epsilon = 2.414 \times 10^4\ M^{-1}\ cm^{-1}$.

Relative scalings of $\Delta\epsilon$ at other concentrations of $[TMX_T]$ were obtained from the relative values implied by the linear regression curve for $\Delta\epsilon(570)$ shown in Fig. 1. Since all TMX difference spectra were found to have a single shape in the in vitro calibrations, use of the relative scaling observed for $\Delta\epsilon(570)$ should apply equally well for all pairs of interference filters.

Calibration of active ΔA signals in terms of $\Delta[Ca^{2+}]$. ΔA signals were also calibrated in terms of the underlying change in myoplasmic free $[Ca^{2+}]$ under the assumption that there was no kinetic delay between $\Delta[Ca^{2+}]$ and ΔA. For these relatively low affinity purpurate indicators and for ΔA's on a millisecond time scale this kinetic assumption is very likely to be accurate (cf. Maylie et al., 1987*c*; Hirota et al., 1989). The first step was to calculate $\Delta f\ (=\Delta[CaD]/[D_T])$, the change in the fraction of indicator in the Ca^{2+}-bound form, from the estimates of $\Delta[CaD]$ and $[D_T]$ obtained as described above. $\Delta[Ca^{2+}]$ then follows from Eq. 1 once K_d and the resting value of f are specified.

In the case of PDAA, essentially all of the indicator appeared to be in the Ca^{2+}-free form in fibers at rest (cf. Results and Fig. 4 *A*); thus, resting f was taken to be 0. K_d was taken to be 0.87 mM, the value determined from our in vitro measurements.

In the case of TMX, calculation of $\Delta[Ca^{2+}]$ from Δf was more complicated because of several effects. Since the effective K_d for the Ca^{2+}-TMX reaction in vitro varied with $[TMX_T]$ (cf. Fig. 1), it was necessary to select the value of K_d appropriate to the value of $[TMX_T]$. However, the appropriate value of $[TMX_T]$ was questionable because of the finding mentioned above, that on average only 0.93 $[TMX_T]$ in resting fibers appeared to be in the Ca^{2+}-free form. This fraction suggests that, on average, at most 0.93 of the indicator was in the myoplasm and thus available to react with $[Ca^{2+}]$. (This conclusion follows, since resting myoplasmic $[Ca^{2+}]$ is expected to be ≤ 0.1 μM and hence the fraction of myoplasmic TMX [or PDAA] in the Ca^{2+}-bound form at rest should be $\leq 10^{-4}$.) It thus seemed reasonable to adopt the approach of Maylie et al. (1987*c*) that a more relevant value of indicator concentration to assume for estimation of Δf was the concentration of indicator that appeared to be in the Ca^{2+}-free form at rest. Hence, we have used 0.93 times the measured value of $[TMX_T]$ as the value of $[TMX_T]$ to calibrate $\Delta[Ca^{2+}]$. (As noted by Maylie et al. [1987*c*], this procedure might still overestimate the actual relevant value of $[TMX_T]$ since not all of the TMX in the putative high Ca^{2+} compartment [e.g., the sarcoplasmic reticulum] is expected to be complexed with Ca^{2+}.) The value of K_d for the Ca^{2+}-TMX calibration was taken from the appropriate regression line in Fig. 1 at the calculated value of $0.93[TMX_T]$.

Statistical tests. Unless stated otherwise, results collected from more than two experiments of the same kind are reported as mean ± SEM. For comparison of results from different kinds of experiments, the two-tailed t test was used.

RESULTS

Absorbance Signals from Resting Fibers

Resting dichroic signals from PDAA and TMX. Dye-related absorbance levels (denoted by A_0 and A_{90}) were measured with two forms of linearly polarized light oriented, respectively, parallel and perpendicular to the fiber axis (cf. Baylor et al., 1986). Thus, it was possible to estimate the amplitude of dye-related "dichroic" signals, defined as $A_0 - A_{90}$. Such signals, if present, are presumed to arise from indicator molecules bound to oriented structures within the fiber (cf. Baylor et al., 1982*a*).

With PDAA, $A_0 - A_{90}$ was measured at 508 nm and found to be essentially zero. On average (32 runs from 14 fibers) $A_0 - A_{90}$ was $<1\%$ (range, -7 to $+6\%$) of $(A_0 + A_{90})/2$. Similarly, with TMX, $A_0 - A_{90}$ measured at 521 nm was very close to zero, on average (7 runs on 4 fibers) 3% (range, 0–7%) of $(A_0 + A_{90})/2$. These average values are essentially the same as those reported previously for cut fibers (Maylie et al., 1987*c*; Hirota et al., 1989). In the remainder of the paper we have calculated all dye-related absorbances at wavelength λ, $A(\lambda)$, as the mean value of the two polarized absorbances, i.e., $(A_0(\lambda) + A_{90}(\lambda))/2$.

Apparent diffusion constants of PDAA and TMX in myoplasm. In the cut fiber preparation the steady-state concentrations of both PDAA and TMX, if measured within the central region of a fiber, were found to be greater than the concentration of indicator in the end-pool solutions. From the extent of accumulation of dye within the fiber, an estimate of the percentage of indicator apparently bound to myoplasmic constituents can be made. For PDAA and TMX these estimates were 19 and 27%, respectively (Maylie et al., 1987*c*; Hirota et al., 1989).

A quantitative estimate of indicator binding may also be made in intact fibers from measurements of the dye's apparent diffusion constant (denoted by D_{app}) along the fiber axis (Baylor et al., 1986; Baylor and Hollingworth, 1990). However, to estimate indicator binding from D_{app}, some estimate of the indicator diffusion constant in the absence of binding is required (see below). Additionally, since intact fibers are usually injected with a fixed quantity of dye at a point source, analysis of the absorbance data collected along the fiber axis provides information about the possible disappearance of dye from the fiber during the course of an experiment. To these ends, measurements of $A(508)$ (for PDAA) or $A(521)$ (for TMX), quantities proportional to total dye concentration, were made at different distances along the fiber axis and at different times after dye injection.

The analysis of these data followed that of Baylor et al. (1986) and used the solution to the one-dimensional diffusion equation (Crank, 1956):

$$[D_T](x, t) = \frac{M}{2\sqrt{\pi D_{app} T}} \exp\left[-x^2/(4 D_{app} t)\right] \quad (2)$$

In Eq. 2, $[D_T]$ (x,t) denotes total dye concentration estimated from the measurement of $A(\lambda)$ at distance x from the site of dye injection and time t after injection; D_{app} denotes the apparent longitudinal diffusion constant (in $cm^2\ s^{-1}$); and M denotes the total quantity of dye, referred to fiber cross-sectional area, contained within the fiber ($\mu mol\ cm^{-2}$). Under the assumption that a rapid equilibrium exists between bound

and free dyes, the value of D_{app} should be related to the actual diffusion constant, D, of the indicator, according to the relation

$$D_{app} = \frac{D}{(1 + R)}$$

if R, the ratio of bound to freely diffusible dye, is a constant (Crank, 1956).

Fig. 2, *A* and *C*, shows examples of the measurements and analysis applied to a

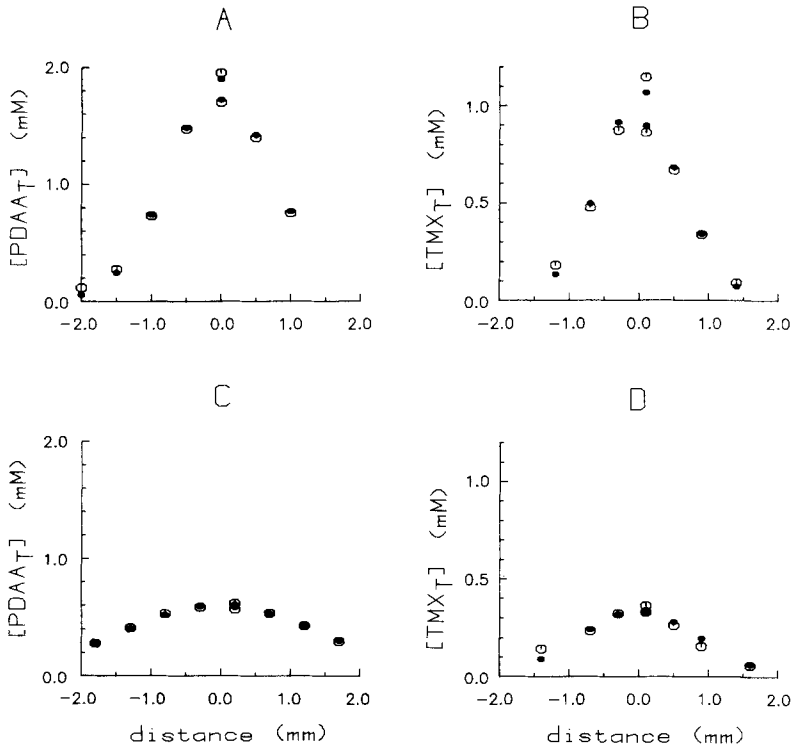

FIGURE 2. (*A* and *C*) Concentration of PDAA within a fiber (ordinate) at different axial distances (abscissa) from the site of dye injection (=location 0 mm). (*B* and *D*) Similar, but for a fiber containing TMX. *Open circles,* values of [D_T] estimated from Beer's law and the measured values of A(508) (for PDAA) or A(521) (for TMX); *filled circles,* best fit of Eq. 2 after adjustment of D_{app} and M. Fiber reference for PDAA: 020189.1; sarcomere length, 3.8 μm; fiber diameter, 102 μm; spot diameter, 73 μm; 16.0°C. Fiber reference for TMX: 122888.2; sarcomere length, 3.8 μm; fiber diameter, 92 μm; spot diameter, 57 μm; 16.1°C. Times after dye injection were 40–49 min (*A*), 23–33 min (*B*), 179–191 min (*C*), and 67–74 min (*D*). See Table I for fitted values of D_{app} and M.

fiber injected with PDAA. In *A* the estimates of [PDAA$_T$] (*open circles*) were made 40–49 min after dye injection, whereas in *C* the measurements were made 179–191 min after injection. The filled circles show the fits of these data by Eq. 2. In both parts the data were well fitted after least-squares parameter adjustment, with the best-fit values for D_{app} and M being, respectively, 1.08×10^{-6} cm^2 s^{-1} and 0.342 μmol cm^{-2}

(*A*) and 0.96 × 10^{-6} cm^2 s^{-1} and 0.219 μmol cm^{-2} (*C*). The substantial change (36%) in the fitted value of *M* will be discussed in the next section.

According to the measurements of Kushmerick and Podolsky (1969), which were carried out on skinned frog fibers, in the absence of binding a molecule the size of PDAA (mol wt 380) is expected to have an actual myoplasmic diffusion constant (denoted by *D*) of ~1.74 × 10^{-6} cm^2 s^{-1} at 16°C. Given this value of *D* and the average value of D_{app} obtained in Fig. 2, *A* and *C*, Eq. 3 suggests that 41% of the indicator was bound to large and relatively immobile myoplasmic constituents. A second estimate of dye binding may be obtained from the value of *D* estimated for PDAA in the cut fiber experiments of Hirota et al. (1989), where the average values of the measured parameters D_{app} and *R* were 1.07 × 10^{-6} cm^2 s^{-1} and 0.23, respectively (16°C). These measurements imply (cf. Eq. 3) a value for *D* of 1.31 × 10^{-6} cm^2 s^{-1}. If the latter value is assumed to apply to our intact fibers, Eq. 3 and the average of the fitted values of D_{app} from Fig. 2, *A* and *C*, suggest that 22% of the PDAA was bound in this experiment.

Column 4 of Table I (part *A*) summarizes information about D_{app} for PDAA as obtained in similar fits from five fibers. The average value of D_{app}, 0.99 × 10^{-6} cm^2 s^{-1}, suggests that 24–43% of the PDAA in myoplasm was bound, corresponding, respectively, to the estimates of *D* obtained from the work of Hirota et al. (1989) and Kushmerick and Podolsky (1969). These estimates are somewhat larger than the 19% bound percentage estimated for PDAA in cut fibers, where the average value of D_{app}, 1.07 (±0.05) × 10^{-6} cm^2 s^{-1}, was slightly, but not significantly, larger than that reported here for intact fibers.

Fig. 2, *B* and *D*, shows an analogous experiment for a fiber injected with TMX, and column 4 of Table I (part *B*) shows the fitted values of D_{app} obtained in four similar experiments. On average, D_{app} was 0.98 (±0.07) × 10^{-6} cm^2 s^{-1}. This average value suggests that 44–50% of the TMX in myoplasm was bound, corresponding, respectively, to the estimates of *D* obtained from the work of Maylie et al. (1987*c*) and Kushmerick and Podolsky (1969). Again, these estimates are somewhat larger than the 27% bound percentage estimated for TMX in cut fibers.

In contrast to the PDAA results, our average value of D_{app} for TMX in intact fibers, 0.98 (±0.07) × 10^{-6} cm^2 s^{-1} (at 16°C), is significantly smaller ($P < 0.05$) than that reported in cut fibers by Maylie et al. (1987*c*), 1.27 (±0.06) × 10^{-6} cm^2 s^{-1} at a similar temperature (17.9°C). The finding of a smaller average value of D_{app} in intact compared with cut fibers was also observed previously with four other absorbing compounds: arsenazo III, antipyrylazo III, phenol red, and horse myoglobin (Baylor et al., 1986; Maylie et al., 1987*a*, *b*; Baylor and Pape, 1988; Irving et al., 1989; Baylor and Hollingworth, 1990). The origin and significance of this general trend is not clear, but averaged over the six common compounds (including PDAA) the ratio of D_{app} in intact fibers to that in cut fibers is 0.72 (±0.06, SEM).

The data in column 4 of Table I (parts *A* and *B*) suggest that within any one experiment the estimated value of D_{app} is smaller if the estimate is obtained from measurements taken later in the experiment. A decrease in D_{app} as a function of measurement time was previously reported with antipyrylazo III, in both intact (Baylor et al., 1986) and cut (Maylie et al., 1987*b*) fibers. The origin and significance of this observation is also unclear. One proposal is that the change in D_{app} reflects a

TABLE I

Estimation of the Apparent Diffusion Constant of Purpurate Dyes in Intact Muscle Fibers

Fiber	Time	Average $[D_T]$ at injection site	D_{app}	M	τ
	min	*mM*	10^{-6} *cm*^{2}*s*$^{-1}$	μ*mol cm*$^{-2}$	*min*
(*1*)	(*2*)	(*3*)	(*4*)	(*5*)	(*6*)
(*A*) PDAA					
012789.3	36–51	0.98	0.86	0.161	
012789.4	37–46	2.54	1.08	0.464	240
	78–87	1.57	1.01	0.391	
012889.1	34–46	2.40	1.10	0.464	500
	107–124	1.48	1.07	0.399	
020189.1	40–49	1.82	1.08	0.342	274
	108–119	0.93	0.99	0.269	
	179–191	0.59	0.96	0.219	
	330–340	0.25	[0.70]	[0.116]	
020189.2	41–51	0.55	0.90	0.093	
Mean (n = 5)			0.99*		338
(± SEM)			(± 0.04)		(± 82)
(*B*) TMX					
122888.2	23–33	1.01	(1.09)	0.150	59
	67–74	0.35	0.90	0.073	
122988.2	30–38	0.58	1.21	0.101	41
	67–75	0.19	1.02	0.041	
122988.3	21–27	0.61	(1.02)	0.082	37
	52–57	0.19	0.83	0.036	
122988.4	35–42	0.72	1.06	0.122	
Mean (n = 4)			0.98*		46
(± SEM)			(± 0.07)		(± 7)

The table is based on least-squares fits of Eq. 2 to the indicator concentration data measured at different times after injection and distances from the injection site; for each run, 6–11 measurements of $[D_T]$ were made (cf. Fig. 2). Column *1* gives the fiber identification; column *2*, the times after injection; column *3*, the average indicator concentration measured at the injection site during the run. Columns *4* and *5* show the fitted values of the parameters in Eq. 2: D_{app} (the apparent diffusion constant) and M (proportional to the total amount of indicator injected into the fiber). Column *6* gives, for fibers having more than one run, the least-squares estimate of τ, the time constant for decay of the value of M (cf. text and Fig. 3). In column *4*, part *B*, the values of D_{app} within parentheses may be artifactually high because at times earlier than ~30 min after injection the initial longitudinal spread of indicator owing to the pressure injection may slightly elevate the fitted value of D_{app} (cf. Baylor et al., 1986). In columns *4* and *5*, part *A*, the values within brackets for fiber 020189.1 may be less reliable than the other values for this experiment because at the very late time of the fourth run the indicator's concentration profile was spread out and somewhat noisy. For the PDAA experiments (part *A*), sarcomere lengths varied between 3.8 and 4.1 μm; fiber diameters, between 71 and 101 μm; and bath temperatures between 16.1 and 16.2°C. For the TMX experiments (part *B*), sarcomere lengths varied between 3.7 and 3.8 μm; fiber diameters, between 92 and 118 μm; and bath temperatures between 16.1 and 16.2°C.

*Each fiber contributed one value to the calculation of means and SEMs of D_{app}; the value used for each fiber was the average D_{app} for runs taken 0.5–2 h after injection.

reversible but saturable binding reaction of the indicator with some myoplasmic component(s) (Baylor et al., 1986); a second proposal is that both reversible and irreversible binding reactions occur (Maylie et al., 1987*b*).

Significance of the estimates of M. In Fig. 2 the fitted value of M (proportional to the total amount of indicator within the fiber) was smaller if determined later in the experiment, for both PDAA (*A* and *C*) and TMX (*B* and *D*). Table I shows that a similar finding was observed in the other experiments as well. In fact, with TMX the decrease in the indicator concentration at late times in the experiment, due both to loss of indicator from the fiber and to diffusion along the fiber, made it difficult to reliably measure $A(\lambda)$ and M at times later than 80–90 min after injection. These

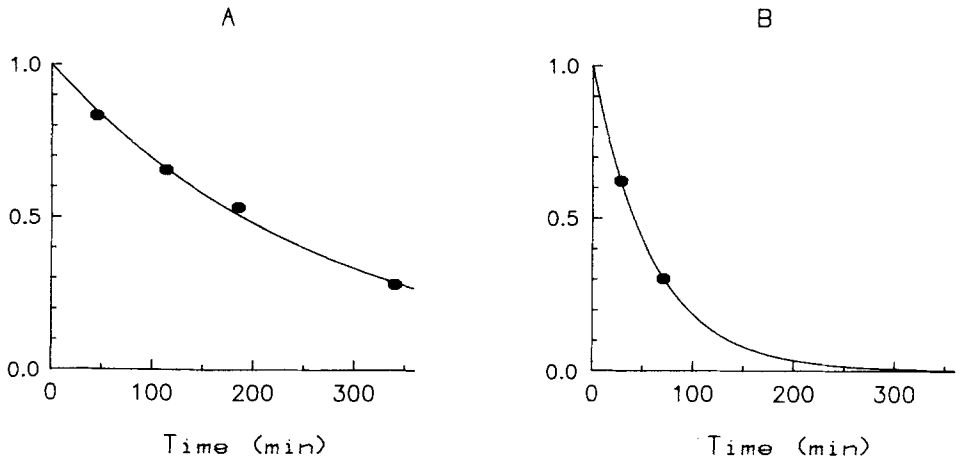

FIGURE 3. Amount of total indicator contained within a single fiber relative to the total amount injected at time $t = 0$ (ordinate) plotted as a function of time after injection (abscissa). *Filled circles,* relative indicator amounts, which are proportional to the variable M in Eq. 2, were obtained from fits of the type shown in Fig. 2. For the abscissa, the specified time t was taken to be the midpoint of the times in the run used for the fitting of M. The curves shown have the functional form $\exp(-t/\tau)$. In each part, the value of τ was obtained by a least-squares fit of the equation $M(t) = M(0)\exp(-t/\tau)$ to the set of values of $M(t)$ available from the experiment. The fitted values of τ and $M(0)$ were, respectively, 274 min and 0.410 μmol cm^{-2} (PDAA-injected fiber, *A*) and 59 min and 0.241 μmol cm^{-2} (TMX-injected fiber, *B*). Same fibers as in Fig. 2.

dramatic decreases in M were not seen previously with three other indicators tested (antipyrylazo III, fura-2, and phenol red), for which the values of M measured at times 50 min or more after the initial estimate were found to decrease by no more than ~5% (Baylor et al., 1986; Baylor and Hollingworth, 1988, 1990).

Under the assumption that the decrease in M for the purpurate indicators follows a first-order process, the data in Table I may be used to estimate the time constant, τ, of the loss. For this estimation, the values of M obtained for any one fiber at different times were fitted by a single exponential function (cf. Fig. 3). The values of τ so estimated are given in column 6 of Table I. In all experiments the values of τ estimated with TMX were smaller than those estimated with PDAA. On average, τ was

46 (±7) min for TMX and 338 (±82) min for PDAA. This nearly eightfold difference is statistically significant ($P < 0.05$).

The most likely explanation for the time-dependent decrease in M is that these purpurate indicators permeate the exterior (surface and/or t-tubular) membranes of the fiber. In the case of TMX this conclusion is perhaps not surprising given the reports of Ogawa et al. (1980) and Maylie et al. (1987*c*) that TMX probably permeates the membranes of the sarcoplasmic reticulum. The finding of a larger τ for PDAA compared with TMX also seems reasonable since PDAA with its two acetate groups has more "localized" charge than does TMX, and therefore PDAA should have a smaller membrane permeability (cf. Ross et al., 1977; Rink et al., 1982).

An alternative interpretation not ruled out by our experiments is that with time both purpurate indicators became chemically altered within the fiber in such a way that the molar extinction coefficient of the compounds decreased. (A third possibility, a photo-bleaching of the dyes during the course of an experiment, seems unlikely since no evidence for photo-bleaching of either TMX or PDAA was found in the in vitro calibrations.)

Resting absorbance spectra of the indicators. In cut fibers, an interesting difference between PDAA and TMX concerned the shape of the absolute absorbance spectra of the indicators. As expected for a low-affinity indicator confined to the myoplasm, PDAA had a resting spectrum indistinguishable from that of dye in a 0 Ca^{2+} environment (Hirota et al., 1989). In contrast, TMX, in spite of an even lower affinity for Ca^{2+}, had a spectrum characteristic of dye partially saturated with Ca^{2+} (on average, 0.13 Ca^{2+} bound; Maylie et al., 1987*c*). The explanation suggested was that Ca^{2+}-free TMX permeates the SR membranes and that roughly 0.27 of the total indicator might be within the SR, a value consistent with the fraction of nondiffusible indicator estimated for TMX; moreover, if free [Ca^{2+}] inside the SR is 1–2 mM (cf. Hasselbach and Oetliker, 1983), roughly half of the indicator inside the SR (i.e., ~0.13 of the total indicator) should then have a spectrum characteristic of Ca^{2+}-bound TMX. In view of these findings it was of interest to measure the resting spectra of PDAA and TMX in intact fibers and to estimate the fraction of each indicator in the Ca^{2+}-bound form.

Fig. 4 *A* (*crosses*) shows the measured values of $A(\lambda)/A(508)$ for a fiber injected with PDAA. For comparison, the two curves show appropriately scaled in vitro absorbance spectra of PDAA in the Ca^{2+}-free and Ca^{2+}-bound forms. The muscle data are well fitted by the 0 Ca^{2+} spectrum. To obtain a quantitative estimate of the fraction of indicator in the Ca^{2+}-bound form, the muscle data were least-squares fitted by a linear combination of the 0 Ca^{2+} and saturating Ca^{2+} spectra. From the relative values of the weighting factors that gave the best fit (+1.005 and −0.005, respectively), it follows that −0.005 of the indicator appeared to be Ca^{2+} bound. (Note that because of noise in the muscle data, a negative fraction might arise in this estimate). Similar fits were carried out in three other fibers at values of [$PDAA_T$] between 0.66 and 3.97 mM. From the four fits the mean fraction of PDAA that appeared to be Ca^{2+} bound was +0.026 (±0.009, SEM), a value not significantly different from zero ($P > 0.05$). A similar conclusion was reached by Hirota et al. (1989) for cut fibers, in which the average value of Ca^{2+}-bound PDAA was −0.011 (±0.033).

Fig. 4 *B* shows analogous results from a fiber injected with TMX. The muscle data

(*crosses*) are shifted slightly from the 0 Ca^{2+} spectrum of the indicator toward the saturating Ca^{2+} spectrum. The best fit of the muscle data with a linear combination of the two in vitro curves suggests that 0.099 of the TMX inside this fiber was in the Ca^{2+}-bound form. Similar fits from six fibers at values of [TMX_T] between 0.85 and 2.25 mM gave a mean value of 0.070 (±0.008) for the fraction of Ca^{2+}-bound TMX. This mean value is significantly greater than zero ($P < 0.01$); it is also significantly less ($P < 0.01$) than the 0.13 (±0.01) values for Ca^{2+}-bound TMX found by Maylie et al. (1987*c*) in cut fibers. Nevertheless, the qualitative conclusion is similar in the two preparations; namely, that a minor but detectable fraction of TMX (but not PDAA) has a spectrum characteristic of Ca^{2+}-bound indicator.

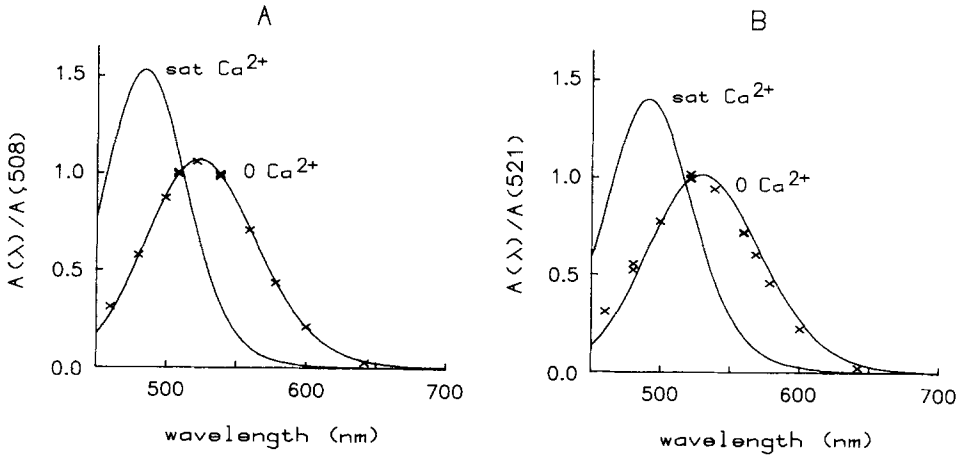

FIGURE 4. In vivo and in vitro absorbance spectra of PDAA (*A*) and TMX (*B*). Crosses indicate the dye-related value of absorbance measured in a resting fiber at the indicated wavelength relative to that measured close to an isosbestic wavelength. The curves show relative spectral shapes for the indicators measured in vitro under Ca^{2+}-free and saturating Ca^{2+} conditions. In each part, the saturating-Ca^{2+} curve (*sat* Ca^{2+}) was obtained by extrapolation; that is, the 0 Ca^{2+} curve was added to a Ca^{2+} difference spectrum scaled to have its saturating amplitude (cf. fits in Fig. 1). (*A*) Fiber reference, 012789.4; [$PDAA_T$], 3.97 mM; sarcomere length, 4.1 μm; fiber diameter, 71 μm; time after injection, 20–28 min; 16.2°C. (*B*) Fiber reference, 010589.3; [TMX_T], 1.30 mM; sarcomere length, 4.1 μm; fiber diameter, 82 μm; time after injection, 3–10 min; 16.1°C.

Absorbance Changes in Response to a Single Action Potential

Active dichroic signals from the indicators. In response to a single stimulated action potential, dye-related absorbance changes (denoted by ΔA_0 and ΔA_{90}) were measured simultaneously with the two forms of linearly polarized light. Similar to the findings reported above for resting fibers, the dye-related ΔA signals were found to have essentially identical amplitudes with the two polarized forms; with both PDAA and TMX the average value of $|\Delta A_0 - \Delta A_{90}|/[0.5(\Delta A_0 + \Delta A_{90})]$ was ≤ 0.05. In the remainder of this paper any small dichroic signals from the indicators have been ignored and all reported changes are based on an equal weighting of ΔA_0 and ΔA_{90}.

Fibers injected with PDAA. Fig. 5 shows optical signals measured in response to an action potential initiated at zero time from a fiber region containing 1.14 mM PDAA. The upper four traces in Fig. 5 *A* show the raw transmission changes recorded at the wavelengths indicated in nanometers to the left. The bottom trace (labeled ΔB) shows the average of the two intrinsic birefringence signals recorded just before and just after the four transmission records shown. The early downward component of ΔB (peak value, -1.7×10^{-3} $\Delta I/I$; time to peak, 8 ms) is characteristic of that seen in healthy fibers at long sarcomere length (cf. Methods).

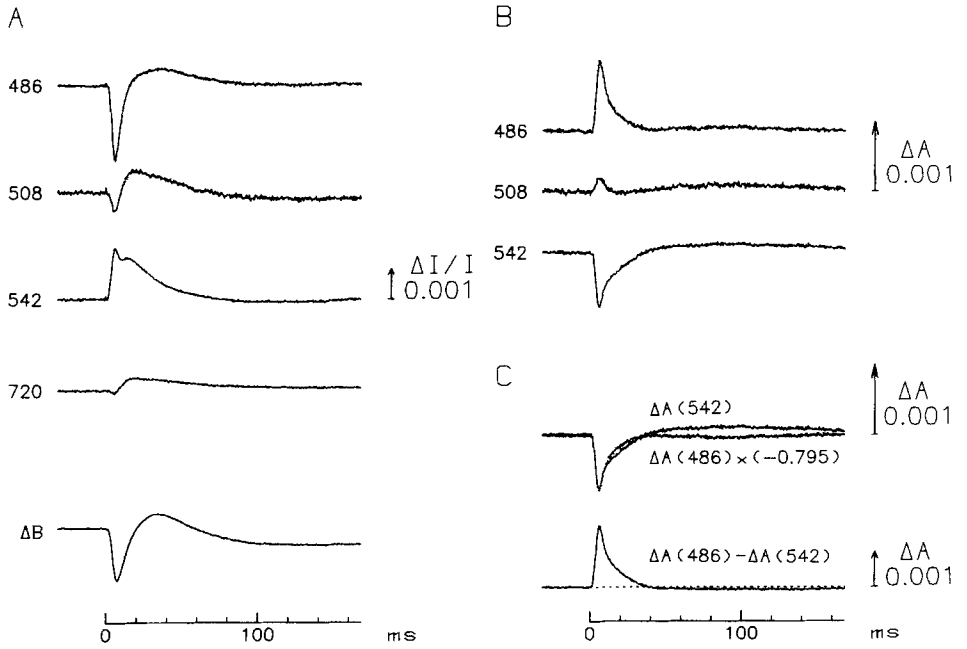

FIGURE 5. Optical signals recorded in response to a single stimulated action potential from a fiber region containing 1.14 mM PDAA. Zero time marks the moment of the external shock. (*A*) Original records of transmission changes at the wavelength, in nanometers, indicated to the left (upper four records) and the intrinsic birefringence signal (ΔB) recorded with 700-nm illumination. The transmission changes were measured with a spot of light (diameter = 73 μm at the fiber) focused near the site of dye injection. The birefringence signal was measured from the 300-μm field of view seen by the microscope objective, centered on the injection site. The calibration bar applies to all five records. Wide-band filters were used, except for the 508-nm trace, which was taken with a narrow-band filter. Each record is an average of two sweeps. During the run, the average value of $A(508)$, the dye-related absorbance in the resting state, was 0.113. (*B*) Dye-related absorbance changes, obtained at the indicated wavelengths from the records in *A* by the procedure described in the text. (*C*) *Upper,* superposition of the 542- and 486-nm absorbance changes from *B* after the indicated scaling of the 486-nm trace; the factor −0.795 was obtained from a least-squares fit of the two traces through time to peak. *Lower,* result of subtraction of the 542-nm ΔA from the 486-nm ΔA. As described in the text, traces of this type were routinely used to estimate $\Delta[Ca^{2+}]$ during the twitch. The dashed baseline represents no change in absorbance. Fiber reference, 022789.1; sarcomere length, 4.0 μm; fiber diameter, 104 μm; time after injection, 7–9 min; 16.1°C.

In Fig. 5 *A* the transmission change at 720 nm, a wavelength at which contributions from PDAA's ΔA should not contribute (cf. Fig. 4 *A*), is characteristic of that observed in highly stretched fibers in which effects due to motion artifacts have been nearly eliminated. This signal, scaled by the factor $(720/\lambda)^{1.6}$ (Hollingworth and Baylor, 1990), was used to estimate and remove the intrinsic intensity change at a shorter wavelength λ, thus permitting an estimate of the dye-related change. Fig. 5 *B* shows the result of this correction. (Note that the calibration bar in Fig. 5 *B* has been adjusted by the factor $-\log_e 10$, which relates fractional intensity changes to absorbance changes.) As expected for a Ca^{2+}-related ΔA from this indicator, the signals in Fig. 5 *B* show a transient decrease in absorbance at 542 nm, a transient increase in absorbance at 486 nm that is somewhat larger in absolute value than the 542-nm signal, and a relatively small change at 508 nm, a wavelength close to the isosbestic wavelength of the indicator (511 nm; cf. Fig. 4 *A*).

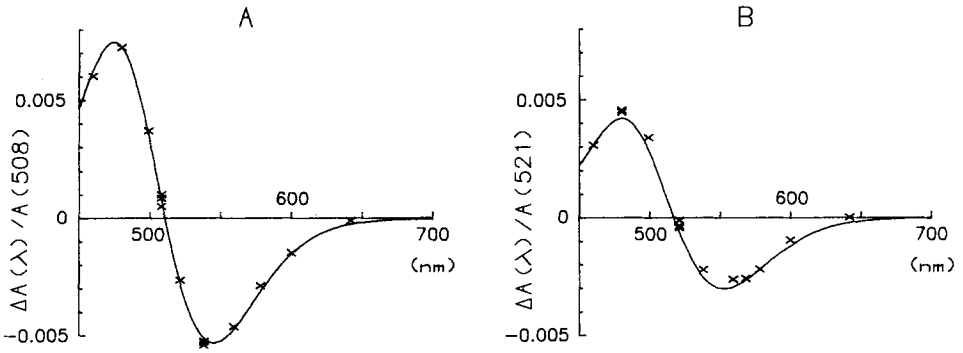

FIGURE 6. *Crosses*, peak values of the absorbance change recorded at different wavelengths in response to a single action potential from a fiber injected with PDAA (*A*) and a second fiber injected with TMX (*B*). For the ordinate in each part, the dye-related ΔA at the indicated wavelength (abscissa) has been normalized by the value of resting absorbance recorded near an isosbestic wavelength. The curves are Ca^{2+} difference spectra obtained in vitro and scaled to provide a least-squares fit to the muscle data. According to the calibration constants given in Methods, the peak value of $\Delta[Ca^{2+}]$ for the fiber in *A* was 7.2 μM, whereas in *B* it was 18.2 μM. Same fibers and runs as in Fig. 4.

In Fig. 5 *C* the upper pair of traces shows a superposition of the $\Delta A(542)$ and $\Delta A(486)$ traces from Fig. 5 *B*; the $\Delta A(486)$ trace has been scaled so as to provide a best fit to the $\Delta A(542)$ waveform. Through time to peak and partly into the falling phases the shapes of the two traces are identical, as expected if both ΔA's monitor the change in myoplasmic free $[Ca^{2+}]$. At later times in the transient the signals diverge, indicating that there is a contamination from a non-Ca^{2+} component in either or both of the signals. For example, a movement-related component may contaminate both $\Delta A(542)$ and $\Delta A(486)$ (see also the later phase of the 508-nm trace in Fig. 5 *B*). If the amplitude of the movement-related component is proportional to $A(\lambda)$, a direct subtraction of the $\Delta A(542)$ trace from the $\Delta A(486)$ trace should nearly eliminate this component (cf. Fig. 4 *A*, which shows that $A(542)$ approximately equals $A(486)$ for PDAA); on the other hand, the Ca^{2+}-related ΔA should summate in a subtraction.

This ΔA "difference" trace is shown as the bottom trace in Fig. 5 *C*. The early peak, if calibrated by Beer's law and the extinction coefficient changes given in Methods, corresponds to the transient formation of 12 μM Ca^{2+}–PDAA complex. At later times the ΔA trace slightly undershoots the baseline, an observation that, as mentioned below, was not consistently seen in the PDAA experiments.

In Fig. 5 *C* the scaling factor (−0.795) that provided a best fit of the $\Delta A(486)$ trace

TABLE II

Analysis of Signals Recorded in Response to a Single Action Potential in Fibers Injected with PDAA

Fiber	$[PDAA_T]$	Time after injection	ΔB		$\Delta[Ca^{2+}]$			$\frac{\Delta A_{steady}}{\Delta A_{peak}}$
			Time to peak	Peak $\Delta I/I$	Time to peak	Half-width	Peak value	
	mM	*min*	*ms*	-10^3	*ms*	*ms*	*μM*	
(1)	*(2)*	*(3)*	*(4)*	*(5)*	*(6)*	*(7)*	*(8)*	*(9)*
012789.3	2.62	6–8	7.2	1.6	6.4	10.5	8.8	+0.01
012789.4	7.14	6–9	9.6	2.0	6.8	10.2	7.2	−0.03
012889.1	5.36	6–8	7.6	1.9	6.0	9.4	12.7	+0.06
020189.1	4.10	8–10	10.4	1.7	9.2	10.5	6.7	—
020189.2	1.22	8–10	8.4	1.7	6.8	8.8	10.6	+0.08
022389.1	1.08	4–6	8.0	2.7	5.6	—	11.5	—
022789.1	1.14	6–9	7.6	1.7	6.0	8.0	9.5	−0.04
022889.1	1.66	7–10	8.4	1.9	6.4	6.9	7.1	−0.05
022889.2	1.27	5–7	—	—	5.4	6.2	9.0	+0.06
022889.3	1.51	6–8	8.4	1.9	6.8	8.1	11.1	−0.04
Mean (±SEM)			8.4 (±0.3)	1.9 (±0.1)	6.5 (±0.3)	8.7 (±0.5)	9.4 (±0.6)	+0.01 (±0.02)

The table summarizes information contained in records of the type shown in Fig. 5, from experiments on PDAA-injected muscle fibers. In general, the earliest run after dye injection was analyzed, corresponding to the run with the largest indicator concentration. Column *1* gives the fiber reference; column *2*, the average value of $[PDAA_T]$ during the run, as estimated from narrow-band measurements of $A(508)$; and column *3*, the time after injection during which the run was made. Columns *4* and *5* give information about the time to peak and peak value, respectively, of the intrinsic birefringence signal recorded at 700 nm during the run; the values given are characteristic of those seen in fibers at this sarcomere length before injection of dye. The remaining columns refer to information obtained from the dye-related ΔA "difference" measurement of the type shown in the lower trace of Fig. 5 *C*, namely, $\Delta A = \Delta A(486) - \Delta A(542)$. Columns *6–8* give, respectively, the time to peak value, the half-width, and the peak change in free $[Ca^{2+}]$ if ΔA is converted to $\Delta[Ca^{2+}]$ by the calibration procedure described in Methods. Column *9* gives the value of ΔA averaged over the interval of 128–168 ms after stimulation divided by the peak value of ΔA. For the 10 fibers, sarcomere lengths varied between 3.8 and 4.1 μm; fiber diameters, between 65 and 104 μm; and bath temperatures, between 16.0 and 16.2°C. A blank in the table signifies that the signal was too noisy or had too much interference from movement artifacts to measure reliably.

to the $\Delta A(542)$ trace is very close to the factor expected for a Ca^{2+}–PDAA signal, namely, −0.813. (This latter factor was estimated from the in vitro $\Delta A(\lambda)$ curves, smoothed appropriately for measurements with the wide-band interference filters.) Fig. 6 *A* (*crosses*) provides a more complete characterization of the wavelength dependence of the ΔA signal from PDAA, obtained from an experiment in which measurements were made with narrow-band filters. The curve in Fig. 6 *A* shows the

least-squares fit of the muscle data by an in vitro Ca^{2+}–PDAA difference spectrum. The close agreement between the in vitro and in vivo shapes provides strong evidence that the muscle ΔA signal is due to the transient binding of Ca^{2+} by PDAA.

Wide-band ΔA signals of the type shown in the lowermost trace in Fig. 5 *C* were generally used to measure $\Delta[Ca^{2+}]$ in our PDAA-injected fibers. Table II summarizes results from 10 experiments. The data in columns *6–8* were obtained from the $\Delta A(486)$–$\Delta A(542)$ signals, calibrated in terms of $\Delta[Ca^{2+}]$ as described in Methods. On average (±SEM), $\Delta[Ca^{2+}]$ reached a peak value of 9.4 (±0.6) μM at 6.5 (±0.3) ms after stimulation; the half-width of the $\Delta[Ca^{2+}]$ was 8.7 (±0.5) ms. At later times in the transient, e.g., 130–170 ms after stimulation, the value of $\Delta[Ca^{2+}]$ was not significantly different from baseline (cf. column 9 of Table II), with an average value of

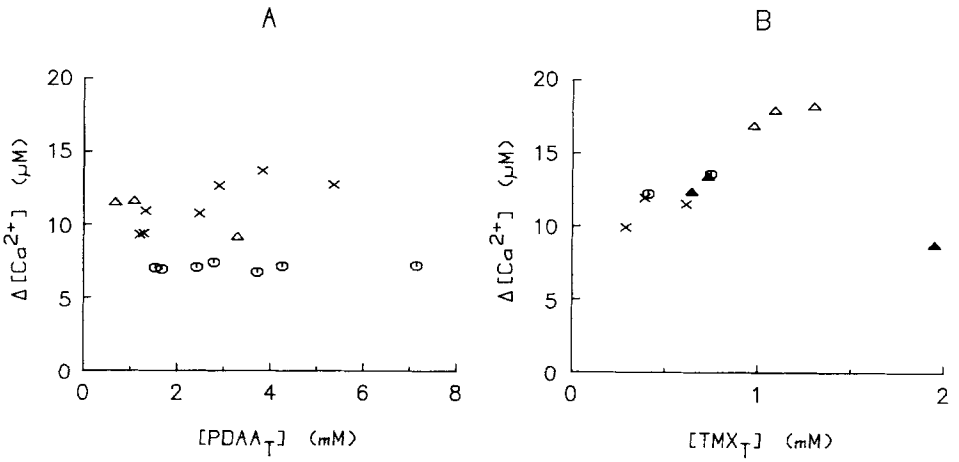

FIGURE 7. Peak value of $\Delta[Ca^{2+}]$ (ordinate) as a function of indicator concentration (abscissa). Within each part, each symbol type corresponds to results obtained from the same fiber. For *B*, the 0.93 scaling factor (cf. Methods) has not been applied to the values of $[TMX_T]$. Fiber identifications were as follows: (*A*) *Crosses,* 012889.1; *circles,* 012789.4; *triangles,* 022389.1. (*B*) *Crosses,* 012689.1; *circles,* 012789.2; *open triangles,* 010589.3; *filled triangles,* 012789.1. See Tables II and III for additional information on each fiber.

+0.01 (±0.02) observed for the ratio of the late ΔA divided by the peak ΔA. This ratio is also not significantly different from the values +0.01 to +0.02 reported with the indicators azo-1 and fura-2 for the ratio of $\Delta[Ca^{2+}]$ measured 150 ms after stimulation to its peak value (Hollingworth and Baylor, 1986; Baylor and Hollingworth, 1988).

The properties of $\Delta[Ca^{2+}]$ inferred from PDAA (Table II) are similar to those reported in cut fibers (Hirota et al., 1989), except for the peak value of $\Delta[Ca^{2+}]$, which at 9.4 (±0.6) μM is about half the value reported in cut fibers, 21 (±1) μM, or 18.8 (±0.9) μM if the ΔA values of Hirota et al. (1989) are calibrated by the constants given in Methods.

Fig. 7 *A* summarizes results from three fibers in which $\Delta[Ca^{2+}]$ was successfully

measured within the same fiber over about a fourfold range of values of $[PDAA_T]$. The peak value of $\Delta[Ca^{2+}]$ (ordinate) showed little or no dependence on indicator concentration (abscissa). The times-to-peak and half-widths of the signals (not shown) also showed little or no variation with $[PDAA_T]$, except for one fiber in which signal half-width increased slightly with indicator concentration, from 7.4 to 10.2 ms for values of $[PDAA_T]$ between 1.53 and 7.14 mM. These results, which are also similar to those reported for PDAA signals in cut fibers (Hirota et al., 1989), are expected if PDAA at millimolar concentrations does not itself affect $\Delta[Ca^{2+}]$.

For two of the fibers in Fig. 7 *A* the measurements of $\Delta[Ca^{2+}]$ were made over a

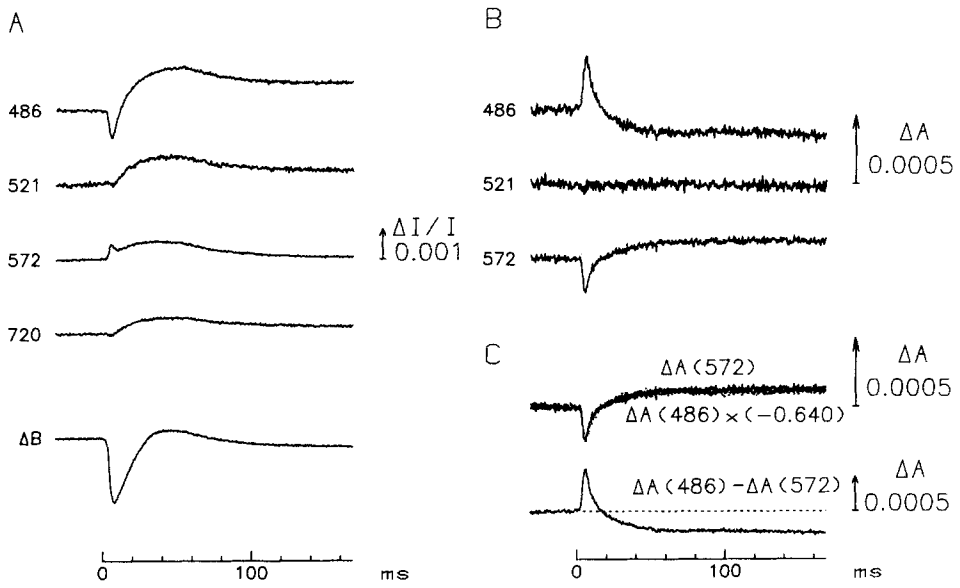

FIGURE 8. Optical signals recorded in response to a single stimulated action potential from a fiber region containing 1.95 mM TMX. Apart from some differences in choice of wavelength, the figure layout is identical to that of Fig. 5. Each record is the average of two to four sweeps. The 521-nm record was obtained with a narrow-band filter; all other records were obtained with wide-band filters. During the run, the average value of $A(521)$ was 0.119. Fiber reference, 012789.1; sarcomere length, 4.0 μm; fiber diameter, 61 μm; time after injection, 3–6 min; 16.0°C.

period long enough (81 min, fiber 012789.4; 118 min, fiber 012889.1) that it was possible to estimate possible changes in peak $\Delta[Ca^{2+}]$ with time. For this analysis the peak data for each fiber were analyzed by linear regression. The slopes of the lines, if normalized by the value of the y intercepts, corresponded to changes in peak $\Delta[Ca^{2+}]$ of −1.3%/h and −13.9%/h, respectively. Similarly small changes were also observed for the changes in half-width of $\Delta[Ca^{2+}]$ with time, −0.3%/h and −3.7%/h, respectively. These changes are small enough to be attributed to a slight fiber run-down; they thus argue against a significant time-dependent effect of indicator on peak $\Delta[Ca^{2+}]$. (For the third fiber in Fig. 7 *A* only three measurements of $\Delta[Ca^{2+}]$ were

made, within a 25-min time period; thus it was not possible to make a meaningful estimate of changes in $\Delta[Ca^{2+}]$ with time for this fiber.)

Fibers injected with TMX. Fig. 8, which has the same general layout as Fig. 5, shows an example of optical signals recorded from a fiber region containing 1.95 mM TMX. In Fig. 8 *B* the dye-related changes are consistent with an early transient increase in the amount of Ca^{2+}–TMX complex, followed by a later, maintained decrease. This biphasic signal is closely similar to that reported for TMX in cut fibers (Maylie et al., 1987*c*).

As shown in Fig. 8 *C*, the relative amplitudes of the TMX-related ΔA recorded at $\lambda = 486$ nm and $\lambda = 572$ nm varied as expected for a Ca^{2+}-related signal. The best-fit scaling constant that related $\Delta A(486)$ to $\Delta A(572)$ was -0.640 (Fig. 8 *C*, *top*), which

TABLE III

Analysis of Signals Recorded in Response to a Single Action Potential in Fibers Injected with TMX

Fiber	$[TMX_T]$	Time after injection	ΔB		$\Delta[Ca^{2+}]$			$\frac{\Delta A_{steady}}{\Delta A_{peak}}$
			Time to peak	Peak $\Delta I/I$	Time to peak	Half-width	Peak value	
	mM	*min*	*ms*	-10^{-3}	*ms*	*ms*	μM	
(1)	*(2)*	*(3)*	*(4)*	*(5)*	*(6)*	*(7)*	*(8)*	*(9)*
010589.2	0.37	5–7	8.0	2.0	5.6	5.7	17.7	—
010589.3	1.30	5–7	7.2	2.0	5.6	5.2	18.2	−0.18
012689.1	0.61	8–10	8.0	2.0	5.2	5.8	11.5	−0.48
012789.1	1.95	3–6	7.6	2.1	5.6	5.4	8.7	−0.51
012789.2	0.75	2–5	7.2	2.3	4.8	4.6	13.6	−0.30
012789.3	0.88	3–7	7.6	1.8	6.0	6.4	11.9	−0.42
Mean			7.6	2.0	5.5	5.5	13.6	−0.38
(±SEM)			(±0.2)	(±0.1)	(±0.2)	(±0.3)	(±1.5)	(±0.06)

The table summarizes information contained in records of the type shown in Fig. 8 from experiments on TMX-injected muscle fibers. The layout of the table is identical to that described for Table II. The ΔA "difference" measurements, from which columns *6–9* were obtained, were based on three filter combinations: narrow-band $\Delta A(480) - \Delta A(559)$, fibers 010589.2 and 010589.3; wide-band $\Delta A(486) - \Delta A(542)$, fiber 012789.3; and wide-band $\Delta A(486) - \Delta A(572)$, the three other fibers. For the six fibers, sarcomere lengths varied between 3.8 and 4.1 μm; fiber diameters, between 61 and 89 μm; and bath temperatures, between 16.0 and 16.2°C.

may be compared to the value -0.641 expected from the in vitro calibrations. Moreover, as shown by the more complete data in Fig. 6 *B* (*crosses*) obtained with narrow-band filters from another fiber, the amplitude of ΔA at different λ agrees closely with a Ca^{2+}–TMX difference spectrum measured in vitro (*curve*).

Table III, which has the same format as Table II, summarizes results from six fibers injected with TMX. The average values for both the time-to-peak (column *6*) and half-width (column 7) of $\Delta[Ca^{2+}]$ are slightly smaller than the corresponding values calculated for PDAA in Table II, although only the difference in half-widths is statistically significant ($P < 0.05$). As pointed out by Maylie et al. (1987*c*), a slightly earlier peak and briefer half-width is to be expected for the TMX signal in comparison with that of $\Delta[Ca^{2+}]$ itself if the ΔA waveform has a contribution from a

later component with a polarity opposite that of the main component. (The later component is presumed to reflect events other than the myoplasmic $\Delta[Ca^{2+}]$; see below.)

The peak value of $\Delta[Ca^{2+}]$ (column *8* of Table III) was, on average, 13.6 (±1.5) μM, a value somewhat smaller than, but not significantly different from ($P > 0.05$), the 17.0 (±1.2) μM value reported for four cut fibers that contained TMX at concentrations between 1.75 and 3.14 mM. Moreover, if the ΔA data of Maylie et al. (1987*c*) are converted to $\Delta[Ca^{2+}]$ by the same calibration constants used for Table III, the peak value of $\Delta[Ca^{2+}]$ for their four fibers becomes 12.9 (±1.7) μM, a result essentially identical to that given in Table III.

In five of the six fibers in Table III a reversal in the polarity of the ΔA signal was seen at late times; in the other fiber, at small $[TMX_T]$, estimation of the ΔA amplitude at late times was not attempted because of an obvious interference from a movement artifact. The average value of the maintained ΔA relative to that of the peak ΔA was −0.38 (±0.06, SEM) (column 9 of Table III), a value significantly different from zero ($P < 0.01$), but not significantly different from the −0.53 (±0.04, SEM) value given by Maylie et al. (1987*c*) for the undershoot of the TMX signal in cut fibers. As pointed out by Maylie et al. (1987*c*), this late, reverse-polarity signal probably reflects a decrease in bound Ca^{2+} for the fraction of TMX (presumed to be in the SR) that has a resting spectrum characteristic of indicator in the Ca^{2+}-bound form.

Fig. 7 *B* plots the amplitude of the early peak $\Delta[Ca^{2+}]$ as a function of $[TMX_T]$ for four fibers. If measured within the same fiber, peak $\Delta[Ca^{2+}]$ showed no consistent dependence on indicator concentration, as was observed for PDAA (Fig. 7 *A*). Again, this result is expected if millimolar concentrations of the indicator do not alter $\Delta[Ca^{2+}]$. For any particular fiber in Fig. 7 *B*, the measurements of $\Delta[Ca^{2+}]$ were made within a very brief time period (~5 min), so that it was not possible to estimate any drift in the properties of $\Delta[Ca^{2+}]$ with time (cf. above, where changes in $\Delta[Ca^{2+}]$ for PDAA were estimated).

DISCUSSION

This article describes absorbance signals detected from intact single muscle fibers injected with either of two purpurate indicator dyes, PDAA or TMX. Our results confirm the finding first observed in cut fibers (Maylie et al., 1987*c*; Hirota et al., 1989), that in response to a single action potential the peak value of $\Delta[Ca^{2+}]$ calibrated from PDAA or TMX is 5–10-fold larger than that calibrated previously in the same preparation with higher affinity (and more highly bound) indicator dyes such as antipyrylazo III, azo-1, and fura-2 (cf. Hollingworth and Baylor, 1986; Baylor and Hollingworth, 1988). A somewhat surprising finding is that in intact fibers the calibrated peak value of $\Delta[Ca^{2+}]$ observed with PDAA, 9.4 ± 0.6 μM (±SEM), is only half that reported previously in cut muscle fibers by Hirota et al. (1989), 20.7 ± 1.0 μM (or 18.8 ± 0.9 μM if our value measured for PDAA's K_d for Ca^{2+}, 0.87 mM, is used to calibrate the data of Hirota et al. [1989]). In contrast, the value of $\Delta[Ca^{2+}]$ calibrated with TMX in intact fibers is identical to that found in cut fibers if our calibration procedure (cf. Methods) is applied to the raw data of Maylie et al. (1987*c*) (13.6 ± 1.5 μM for intact vs. 12.9 ± 1.7 μM for cut fibers).

Although we have no explanation why the ratio of peak values of $\Delta[Ca^{2+}]$ detected

in the two preparations should differ according to the indicator used, for a variety of reasons TMX (as used in either intact or cut fibers) should probably be considered a less reliable indicator of $\Delta[Ca^{2+}]$ than PDAA. First, the in vitro calibrations of TMX (cf. Fig. 1) clearly revealed complexity in the titrations with Ca^{2+} that was not seen with PDAA. Second, the percentage of bound (or sequestered) indicator within a fiber was estimated to be somewhat greater for TMX than for PDAA in both cut and intact fibers. Third, the resting spectrum of TMX detected in either preparation indicated that a significant fraction of the indicator (0.07 ± 0.02 in intact fibers; 0.13 ± 0.01 in cut fibers) appeared to be in a high Ca^{2+} environment; in contrast, the analogous fractions in the case of PDAA were not significantly different from zero ($+0.026 \pm 0.009$ in intact fibers; -0.011 ± 0.003 in cut fibers). Fourth, with TMX the waveform of Δ[CaD] detected during fiber activity had a clearly resolved undershoot not likely to be directly related to the myoplasmic $\Delta[Ca^{2+}]$; this signal component was not seen with PDAA.

For these reasons it would seem reasonable to place more confidence in the calibration of $\Delta[Ca^{2+}]$ obtained with PDAA than with TMX in both intact and cut fibers. Thus, the results suggest that the peak of $\Delta[Ca^{2+}]$ in intact fibers is in fact about half that in cut fibers. In retrospect, this conclusion is supported by earlier results obtained with antipyrylazo III, which also suggest about a twofold smaller peak of $\Delta[Ca^{2+}]$ in intact compared with cut fibers, 1.8 ± 0.2 μM (Baylor and Hollingworth, 1988) vs. 3.9 ± 0.2 μM (Maylie et al., 1987*b*). For this latter comparison, both data sets have been calibrated in the same way, namely, with the calibration constants given in Hollingworth et al. (1987) and under the assumptions that myoplasmic free $[Mg^{2+}]$ is 1.5 mM and that the indicator's ΔA tracks $\Delta[Ca^{2+}]$ with a 1.4-ms kinetic delay (cf. Baylor et al., 1985).

Several explanations may be proposed as to why $\Delta[Ca^{2+}]$ in intact fibers might be smaller than in cut fibers. First, the measurements summarized in Tables II and III were made near the site of dye injection; consequently, if the injection procedure itself produces some fiber damage, the peak value of $\Delta[Ca^{2+}]$ might be smaller than would be measured in the absence of damage. However, in our experiments the intrinsic birefringence signal (a signal closely related to $\Delta[Ca^{2+}]$; cf. Methods) was essentially unchanged by the injection process; this finding argues strongly against the possibility of a significant change in $\Delta[Ca^{2+}]$ due to injection damage or to a pharmacological effect of the indicator. A second possibility concerns the degree of stretch of the fibers. As shown in the following paper (Konishi et al., 1991), at the long sarcomere lengths usually used for indicator dye studies, $\Delta[Ca^{2+}]$ is slightly smaller than that observed at more physiological sarcomere lengths. However, there was no significant difference in sarcomere lengths for the fibers in our study vs. that of Hirota et al. (1989) (3.8–4.1 μm vs. 3.7–4.2 μm, respectively). A third possibility is related to our use of a high Ca^{2+} Ringer's solution (11.8 mM $CaCl_2$) compared with the normal Ringer's solution of Hirota et al. (1.8 mM $CaCl_2$). As is also shown in the following paper (Konishi et al., 1991), a negligible difference is expected in the amplitude of $\Delta[Ca^{2+}]$ due to this difference in Ringer composition. A fourth possibility concerns the way in which the indicator that is bound to myoplasmic constituents may respond to $\Delta[Ca^{2+}]$. Although we cannot rule out this possibility with certainty, it seems unlikely that the relatively minor differences detected in the

percentages of bound indicator (for PDAA, 19% in Hirota et al., 1989 vs. 24–43% in this study; for antipyrylazo III, ~75% in both Maylie et al., 1987*b* and Baylor et al., 1986) could explain a factor of two difference in the calibrated amplitude of $\Delta[Ca^{2+}]$. A final possibility, which is the one we consider to be the most probable, is that $\Delta[Ca^{2+}]$ in cut fibers is abnormally large because of some alteration in the internal physiological state of cut fibers (cf. Irving et al., 1987). In this regard it is of interest to note that the myoplasmic pH transient measured with phenol red in response to action potential stimulation is also larger, by 1.5–3-fold, in cut fibers (Irving et al., 1989) than in intact fibers (Hollingworth and Baylor, 1990).

Advantages and Disadvantages of PDAA as a Ca^{2+} Indicator in Skeletal Muscle

In agreement with Hirota et al. (1989), we conclude that PDAA has some significant advantages in comparison with other Ca^{2+} indicator dyes used previously in muscle. First, because PDAA's K_d for Ca^{2+} is large (~0.9 mM), its absorbance change probably responds to the spatially averaged $\Delta[Ca^{2+}]$ in a linear fashion and without kinetic delay. Second, since the percentage of indicator estimated to be bound to myoplasmic constituents is smaller than that observed previously with other Ca^{2+} indicators, the calibrated value of $\Delta[Ca^{2+}]$ obtained with PDAA is likely to be more accurate. (Whether this value is larger or smaller than the actual value depends on the way in which myoplasmic binding alters the K_d of the indicator, an effect that has not yet been estimated for PDAA.) Third, because of the high selectivity of the indicator for Ca^{2+} over Mg^{2+} and H^+, there should be little of the interference seen from these ions with older generation Ca^{2+} indicators such as arsenazo III and antipyrylazo III.

PDAA also has some disadvantages as an intracellular Ca^{2+} indicator. Because its affinity for Ca^{2+} is low, millimolar concentrations of indicator in myoplasm are required to give a well-resolved signal. Even then, the peak amplitude of ΔA is often only two to three times larger than interfering absorbance changes from movement artifacts and fiber intrinsic changes (cf. Fig. 5). Thus the waveform of $\Delta[Ca^{2+}]$, particularly in its later phases, is subject to the uncertainties of the correction procedure used to remove these signal components. Additionally, the use of millimolar concentrations of indicator raises the possibility that pharmacological effects may influence the physiological processes under study. In the case of PDAA such effects appear to be unimportant, although more substantial effects were detected in the case of DMPDAA (Hirota et al., 1989). A final concern raised by the experiments reported here is that the exterior (surface and/or transverse-tubular) membranes of a muscle fiber appear to have some permeability to PDAA (and an even greater permeability to TMX), since after dye injection the total amount of indicator contained within the fiber decreased with time. If PDAA can also permeate membrane-bound organelles within the fiber, there is the possibility that signal components may arise from the latter compartments and interfere with the interpretation of cytoplasmic $\Delta[Ca^{2+}]$ (although no such effects have been suggested by the experiments either of this article or of Hirota et al., 1989).

As described in the following paper (Konishi et al., 1991), some, but not all, of these disadvantages of PDAA are redressed by the use of furaptra, a recently available fluorescent indicator for Ca^{2+} and Mg^{2+} (Raju et al., 1989).

We thank Dr. W. K. Chandler for a gift of a sample of PDAA, and Dr. Chandler, Dr. S. Hollingworth, Dr. P. C. Pape, and A. B. Harkins for comments on the manuscript.

Financial support was provided by the U. S. National Institutes of Health (grant NS-17620 to S. M. Baylor).

Original version received 12 April 1990 and accepted version received 30 July 1990.

REFERENCES

Baylor, S. M., W. K. Chandler, and M. W. Marshall. 1982*a*. Optical measurements of intracellular pH and magnesium signals in frog skeletal muscle fibres. *Journal of Physiology.* 331:105–137.

Baylor, S. M., W. K. Chandler, and M. W. Marshall. 1982*b*. Use of metallochromic dyes to measure changes in myoplasmic calcium during activity in frog skeletal muscle fibres. *Journal of Physiology.* 331:139–177.

Baylor, S. M., and S. Hollingworth. 1987. Effect of calcium Ca buffering by Fura2 on the second component of the intrinsic birefringence signal in frog isolated twitch muscle fibres. *Journal of Physiology.* 391:90P.

Baylor, S. M., and S. Hollingworth. 1988. Fura-2 calcium transients in frog skeletal muscle fibers. *Journal of Physiology.* 403:151–192.

Baylor, S. M., and S. Hollingworth. 1990. Absorbance signals from resting frog skeletal muscle fibers injected with the pH indicator dye phenol red. *Journal of General Physiology.* 96:449–471.

Baylor, S. M., S. Hollingworth, C. S. Hui, and M. E. Quinta-Ferreira. 1985. Calcium transients from intact frog skeletal muscle fibers simultaneously injected with Antipyrylazo III and Azol. *Journal of Physiology.* 365:70P.

Baylor, S. M., S. Hollingworth, C. S. Hui, and M. E. Quinta-Ferreira. 1986. *Journal of Physiology.* 377:89–141.

Baylor, S. M., and H. Oetliker. 1977. A large birefringence signal preceding contraction in single twitch fibres of the frog. *Journal of Physiology.* 264:141–162.

Baylor, S. M., and P. C. Pape. 1988. Measurement of myoglobin diffusivity in the myoplasm of frog skeletal muscle fibers. *Journal of Physiology.* 406:247–275.

Baylor, S. M., M. E. Quinta-Ferreira, and C. S. Hui. 1983. Comparison of isotropic calcium signals from intact frog muscle fibers injected with Arsenazo III or Antipyrylazo III. *Biophysical Journal.* 44:107–112.

Crank, J. 1956. *The Mathematics of Diffusion.* Oxford University Press, London. 347 pp.

De Mello, W. C. 1973. Membrane sealing in frog skeletal muscle fibers. *Proceedings of the National Academy of Sciences, USA.* 70:982–984.

Hasselbach, W., and H. Oetliker. 1983. Energetics and electrogenicity of the sarcoplasmic reticulum calcium pump. *Annual Review of Physiology.* 45:325–339.

Hirota, A., W. K. Chandler, P. L. Southwick, and A. S. Waggoner. 1989. Calcium signals recorded from two new purpurate indicators inside frog cut twitch fibers. *Journal of General Physiology.* 94:597–631.

Hollingworth, S., R. Aldrich, and S. M. Baylor. 1987. In vitro calibration of the equilibrium constants of the metallochromic indicator dye antipyrylazo III with calcium. *Biophysical Journal.* 51:383–393.

Hollingworth, S., and S. M. Baylor. 1986. Calcium transients in frog skeletal muscle fibers injected with Azo-1. *In* Optical Methods in Cell Physiology. P. DeWeer and B. M. Salzberg, editors. John Wiley & Sons, Inc., New York. 261–263.

Hollingworth, S., and S. M. Baylor. 1990. Changes in phenol red absorbance in response to electrical stimulation of frog skeletal muscle fibers. *Journal of General Physiology.* 96:473–491.

Irving, M., J. Maylie, N. L. Sizto, and W. K. Chandler. 1987. Intrinsic optical and passive electrical properties of cut frog twitch fibers. *Journal of General Physiology.* 89:1–40.

Irving, M., J. Maylie, N. L. Sizto, and W. K. Chandler. 1989. Simultaneous monitoring of changes in magnesium and calcium concentrations in frog cut twitch fibers containing Antipyrylazo III. *Journal of General Physiology.* 93:585–608.

Klein, M. G., B. J. Simon, G. Szucs, and M. F. Schneider. 1988. Simultaneous recording of calcium transients in skeletal muscle using high- and low-affinity calcium indicators. *Biophysical Journal.* 53:971–988.

Konishi, M., S. Hollingworth, A. B. Harkins, and S. M. Baylor. 1991. Myoplasmic calcium transients in intact frog skeletal muscle fibers monitored with the fluorescent indicator furaptra. *Journal of General Physiology.* 97:271–301.

Konishi, M., A. Olson, S. Hollingworth, and S. M. Baylor. 1988. Myoplasmic binding of Fura-2 investigated by steady-state fluorescence and absorbance measurements. *Biophysical Journal.* 54: 1089–1104.

Kovacs, L., R. A. Schumperli, and G. Szucs. 1983. Comparison of birefringence signals and calcium transients in voltage clamped cut skeletal muscle fibres of the frog. *Journal of Physiology.* 341:579–593.

Kushmerick, M. J., and R. J. Podolsky. 1969. Ionic mobility in muscle cells. *Science.* 166:1297–1298.

Maylie, J., M. Irving, N. L. Sizto, and W. K. Chandler. 1987*a*. Comparison of Arsenazo III optical signals in intact and cut frog twitch fibers. *Journal of General Physiology.* 89:41–81.

Maylie, J., M. Irving, N. L. Sizto, and W. K. Chandler. 1987*b*. Optical signals obtained with Antipyrylazo III in cut frog twitch fibers. *Journal of General Physiology.* 89:83–143.

Maylie, J., M. Irving, N. L. Sizto, G. Boyarsky, and W. K. Chandler. 1987*c*. Optical signals obtained with tetramethylmurexide in cut frog twitch fibers. *Journal of General Physiology.* 89:145–176.

Ogawa, Y., H. Harafuji, and N. Kurebayashi. 1980. Comparison of characteristics of four metallochromic dyes as potential calcium indicators in biological experiments. *Journal of Biochemistry.* 87:1293–1303.

Ohnishi, S. T. 1978. Characterization of the murexide method: dual wavelength spectrophotometry of cations under physiological conditions. *Analytical Biochemistry.* 85:165–179.

Palade, P., and J. Vergara. 1982. Arsenazo III and antipyrylazo III calcium transients in single skeletal muscle fibers. *Journal of General Physiology.* 79:679–707.

Raju, B., E. Murphy, L. A. Levy, R. D. Hall, and R. E. London. 1989. A fluorescent indicator for measuring cytosolic free magnesium. *American Journal of Physiology.* 256:C540–C548.

Rink, T. J., R. Y. Tsien, and T. Pozzan. 1982. Cytoplasmic pH and free Mg^{2+} in lymphocytes. *Journal of Cell Biology.* 95:189–196.

Rios, E., and M. F. Schneider. 1981. Stoichiometry of the reactions of calcium with the metallochromic indicator dyes Antipyrylazo III and Arsenazo III. *Biophysical Journal.* 36:607–721.

Ross, W. N., B. M. Salzberg, L. B. Cohen, A. Grinvald, H. V. Davila, A. S. Waggoner, and C. H. Wang. 1977. Changes in absorption, fluorescence, dichroism and birefringence in stained giant axons: optical measurement of membrane potential. *Journal of Membrane Biology.* 33:141–183.

Southwick, P. L., and A. S. Waggoner. 1989. Synthesis of purpurate-1,1′-diacetic acid PDAA tripotassium salt: a new calcium indicator for biological applications. *Organic Preparations and Procedures International.* 21:493–500.

Suarez-Kurtz, G., and I. Parker. 1977. Birefringence signals and calcium transients in skeletal muscle. *Nature.* 270:746–748.

Thomas, M. V. 1979. Arsenazo III forms 2:1 complexes with Ca and 1:1 complexes with Mg under physiological conditions. *Biophysical Journal.* 25:541–548.